# EFFECT OF VACUUM ANNEALING ON THE STRUCTURAL PROPERTIES OF $MOS_2$ SAMPLE

[1]Manuja M,[2]Indu Treesa Jochan,[3]Gijo Jose

[1]Research Scholar,[2]Guest Lecturer,[3]Guide and Assistant Professor,
[1,3]Post Graduate and Research Department of Physics,
[1,3]St. Berchmans College, Changanacherry, Kottayam, India,
[2]Department of Physics, St.Aloysius' College, Edathua, India.

***Abstract :***$MoS_2$ samples were prepared successfully via hydrothermal route. Structural characterizations were performed using X-ray diffraction spectroscopy and Raman spectroscopy. XRD profile confirms the hexagonal phase for the samples and more detailed crystallographic structures were discussed from Rietveld refinement procedure. Expansion of lattice structure with densification of unit cell and decrease in band gap is observed from UV Visible spectroscopy and the stability of phase and structure of 2H $MoS_2$ during vacuum annealing was also studied.

***IndexTerms*–2H$MoS_2$, Rietveld refinement, vacuum annealing.**

## I. INTRODUCTION

Nanotechnology is a brand new technology for the future which is being studied extensively among experimental physicists. The hunt for new application of nanostructured systems is now a major area of research in material science and technology. Transition metal chalcogenides (TMCs) occur with many stoichiometries and structures similar to layered structure as that of graphite.The advantage of TMCs over the graphene is that they have non zero bandgap which can be tuned for an optoelectronic applications. $MoS_2$ attracted considerable attention for its potential advantages in catalysis[1], transistors, batteries, gas sensors, photodetector[2], and other optoelectronic devices[3]. As $MoS_2$ has layered structure[4], the decrease in particle size with reduction in number of layers widens the band gap which results in an increase in transparency of molecule. The tunability of band gap with size and number of layers of nanostructured $MoS_2$ finds applications in solar cell[5]. A thorough investigation has to be done to understand the variation of band gap energy with particle size and number of layers.

BiswanathChakrabortyand co-workers investigated band gap of $MoS_2$ and concluded that it goes from indirect to direct as the bulk $MoS_2$ thinned down to monolayer form[6]. DeepeshGopalakrishnan*et al*[7]. synthesized quantum dots of $MoS_2$, for use in energy-conversion technologies. A study on lattice strain effects on the evolution of the band gap in $MoS_2$nanosheets by D. M. David Jeba Singh *et al*[8], report the correlation between structures of the $MoS_2$nanosheets and their optical properties. According to the work of Matthew D. J. Quinn *et al*[9] size dependent band gap of $MoS_2$ is as high as 2.5 eV in 3D form having size in range of 4-5 nm. In quantum dots, Multiple Exciton Generation (MEG) was also detected in semiconducting single-walled carbon nanotubes (SWNTs) upon absorption of single photon.

In this work we studied the effects of thermal annealing in ultra-high vacuum from room temperature up to 300 °C of two dimensional (2D) hexagonal $MoS_2$ nanostructures. The change in structural and optical properties is noticed with the variation in band gap.

## II. PREPARATION OF SAMPLE

All of the chemical reagents were of analytic purity and used directly without further purification. The ultrathin $MoS_2$ nanostructures were synthesized by a one step hydrothermal reaction using hexa-ammonium hepta-molybdate tetra-hydrate and thiourea as starting materials. In a typical synthesis, 1.24g of hexa-ammonium hepta-molybdate tetra-hydrate and 2.28g of thiourea were dissolved in 36 ml deionized water under vigorous stirring for 30 min to form a homogeneous solution. The solution was then transferred into a 50 ml Teflon lined stainless steel autoclave and sealed tightly heated at 220 $^oC$ or 7h and naturally cooled down to room temperature. Black precipitate were collected by centrifugation and washed with distilled water and absolute ethanol for several times, and finally dried in vaccum at 60$^oC$ for 24h.

*Characterization techniques*

The crystal structure and phase of the sample were investigated through X-ray diffraction technique sing Cu $K_{\alpha 1}$ line of wavelength 1.5406 A˚ using Bruker X-ray diffractometer with in a 2θ value ranges from 5 to 70 ˚ with a step size of 0.02˚. Further structural characterization was performed using Raman spectroscopy measurements of the sample in WITec Alpha300RA (Gmbh Ulm Germany) confocal Raman spectrometer. For this recordings the sample is excited with a monochromatic beam of laser radiation of wavelength 532 nm and having a maximum power of 70 mW. Optical characterizations were performed in the wave length range of 300-900 nm using T90+ UV/Visible spectrophotometer from PG instruments limited.

## III. RESULTS AND DISCUSSION

*X-Ray diffraction spectroscopy*

XRD analysis provides information regarding the intricate aspects of nanostructure including the average grain size[10], including phase purity and crystal structure[11]. Fig.1 (anad b) Shows the X-ray powder diffraction pattern of the sample prepared as such and annealed in vacuum. Obtained data is compared with standard values of JCPDS card number 731508 and found to match with that of hexagonal Molybdenum disulphide with chemical formula $MoS_2$. Peaks at 2θ values at $13.64^0$, $32.29^0$, $35.78^0$, $42.81^0$ corresponds to hkl planes (002), (100), (102), (110) respectively and was found that the peak having maximum intensity corresponds to the (002) plane gives stacking of layers along c axis. The atoms are arranged in the space group P63/mmc. Presence of (100) and (110) confirms the 2H phase of $MoS_2$. The strong characteristic (002) peak is the clear significance of a well–stacked layered structure, and the growth direction is along {00l} phase sets.

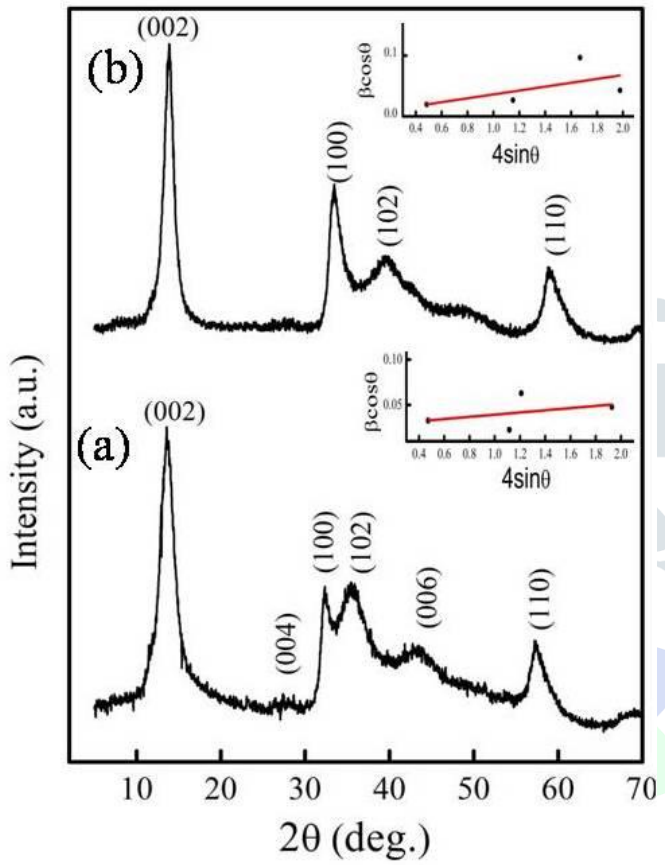


*Fig.1 X-ray diffraction profiles for 2H MoS2 (a) sample prepared as such and (b) annealed at 300 ˚C in vacuum with corresponding W-H plots in the insets.*

The more detailed structural studies were done from Rietveld refinement procedure using Fullprof suit with the help ofpseudovoigit function which is a combination of Gaussian and Lorentzian function[12]. In the hexagonal structure $MoS_2$ is made up of several trigonal prismatic $MoS_6$ units with the second $MoS_6$ unit of 2H $MoS_2$ is turned to 180˚and shown in Fig. 2(a). The third cell is the repetition of first one and the fourth cell will be a repetition of second and so on hence the name 2H $MoS_2$. Corresponding to these, there are two kinds of hexagonal voids and is clearly visualized in fig. 2(b). Fig 2(c) demonstrates the formation of hexagonal channel along the ab plane. The stacking along (002) direction gives the layered nature for the structure with a very weak vanderwaals interaction along c axis between two nearest S atoms of neighbouring $MoS_6$ unit. The detailed bond length and angle representation gives the single Mo-S bond length of 2.3962 Å and the two kinds of bond angle S-Mo-S and Mo-S-Mo of 81.386˚, 82.144˚ and are visualized in Fig 2(d). The structure discussed is in agreement with the work reported earlier [13,14].

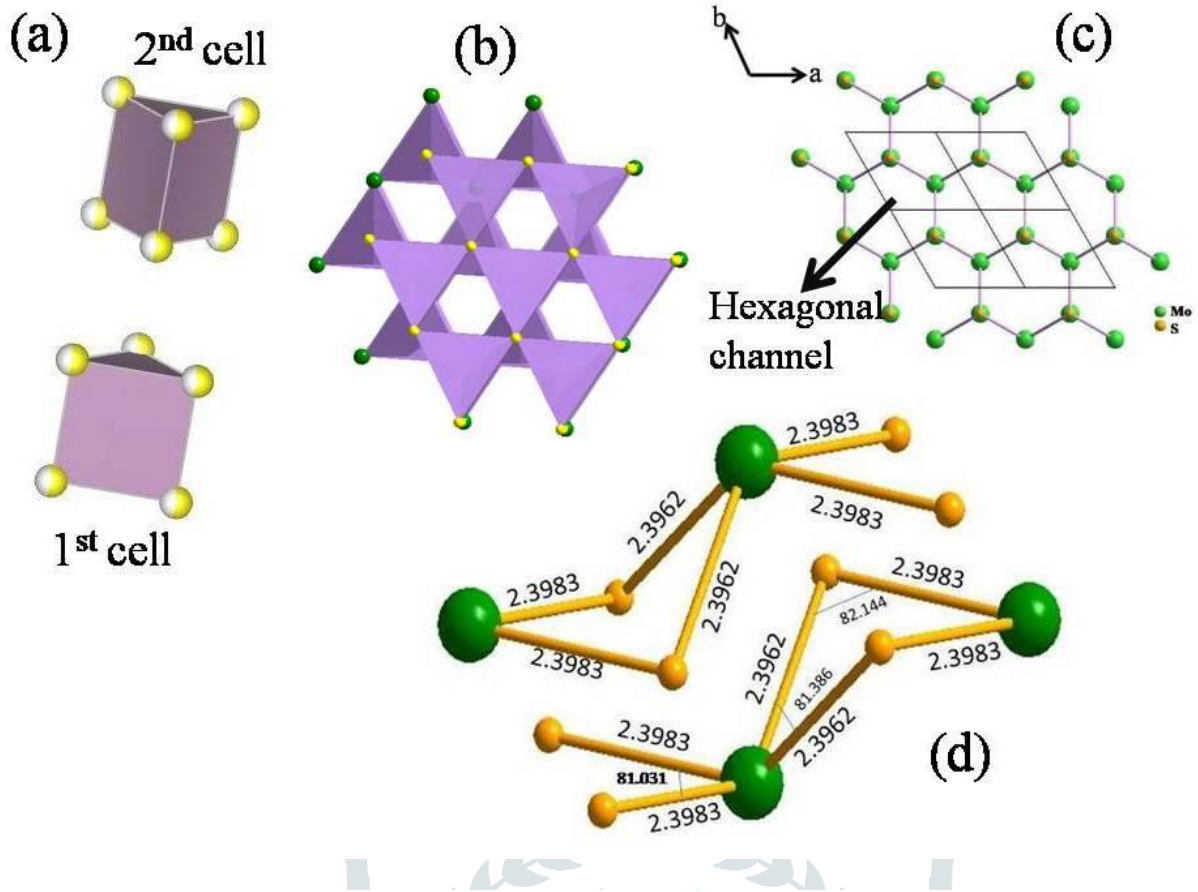


*Fig.2 crystallographic structures for 2H $MoS_2$ obtained from Rietveld refinement procedure (a) polyhedral structures representing two $MoS_6$trigonal prisms (b) polyhedral hexagonal structure representing two kinds of hexagonal voids, (c) hexagonal ring like structure along ab plane and (d) structure showing detailed information regarding bond length and bond angles of 2H $MoS_2$*

The calculation of crystallite size using Debye Scherer's formula $L=K\lambda/\beta\cos\theta$ gives the value 3.87 nm and 4.245nm for samples a and b. In Debye Scherrer equation the broadening of peaks are only due to the crystallite size. But actually this may depend on the lattice strain also following the modified scherrer's equation,

$$\boldsymbol{\beta_{total}}=4\varepsilon\tan\theta+\frac{\mathbf{0.9\lambda}}{\boldsymbol{L\cos\theta}}$$

we can determine the actual crystallite size as well as the lattice stain. To get the more accurate crystallite size and strain influence of the sample, Williamson Hall (WH) plots are taken into account and the respective WH plots for the two samples are given in the inset of Fig. 1 (a and b). Crystallite size calculated from WH Plot is 5.07nm and 6.3 nm respectively for samples a and b and also both shows a tensile nature of lattice strain. From the details of crystallography of hexagonal structure, c values and unit cell volume of both the samples can be calculated using the equation

$$\frac{\mathbf{1}}{\boldsymbol{d^2}}=\frac{\mathbf{4}}{\mathbf{3}}\left(\frac{\boldsymbol{h^2+hk+k^2}}{\boldsymbol{a^2}}\right)+\frac{\boldsymbol{l^2}}{\boldsymbol{c^2}}$$ , a=b and V= $\frac{\sqrt{\mathbf{3}}\boldsymbol{a^2c}}{\mathbf{2}}$

and corresponding c values obtained are 13.02 Å and 13.04 Å with volume $1.1117\times10^{-28}$ $m^3$ and $1.0993\times10^{-28}$ $m^3$ respectively. The difference in c value indicates that sample get expanded during annealing which results in the increase in density.

*Raman spectroscopy*

Raman spectroscopic studies of samples help to derive useful information regarding the optical phonon modes and electron-phonon coupling strength of the sample under study. In order to get detailed insight in to the vibrational bonds in the 2H $MoS_2$ Raman characterizations were performed with an exciting wavelength of 532 nm and the obtained Raman spectra are shown in Fig.3.

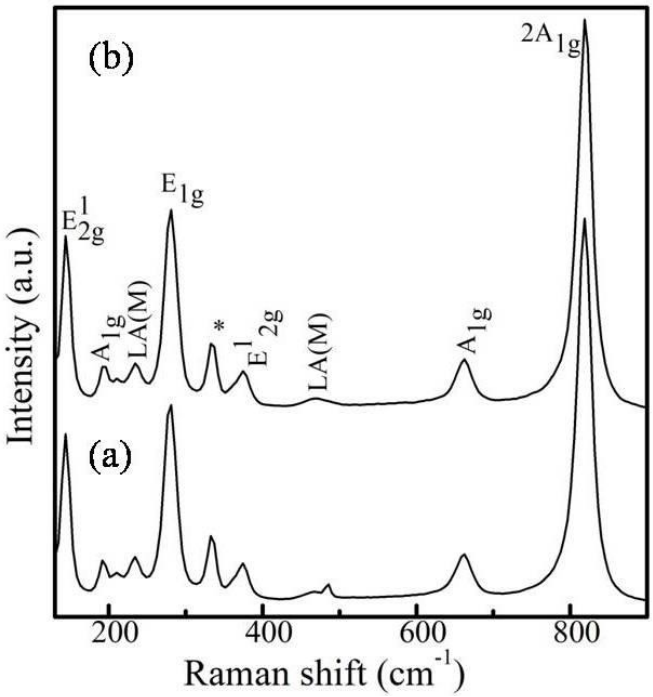


*Fig.3 Raman spectra for 2H $MoS_2$ (a) prepared as such and (b) annealed in vacuum at 300 ˚C*

The Raman peaks are assigned to $E^12g$ mode, $A^1g$ mode, LA (M), E1g and E2g (In plane vibrational) mode of bulk 2H $MoS_2$ crystal, $E^12g$ mode (opposite vibrations of two S atoms with respect to Mo atom), second order 2xLA(M) Scattering process and A1g(M) + LA(M), 2 A1g modes etc at 143, 193, 234, 281, 374, 463, 661 and 819 $cm^{-1}$ regions respectively[15]. Raman shift at 335 $cm^{-1}$ corresponds to partially oxidized $MoS_2$ due to laser power etc. These specific assignments also corresponds to the 2H $MoS_2$ structure.

*UV Visible spectroscopy*

UV absorbance graph is plotted with wavelength along X- axis and absorbance along Y- axis. The wavelength ranges from 200 to 900 nanometers. The optical energy gap is associated with the degree of structural order and disorder of the materials in a medium range. The order/disorder ratio leads to different defect densities in the material which results in different distribution of intermediate levels of energy between the valance (VB) band and conduction band (CB).The optical band gap energy (*Eg*) was estimated by the Tauc plot. Fig.4 gives the tauc plots for the samples and the lower inset shows the corresponding absorbance spectra for the material under investigation.

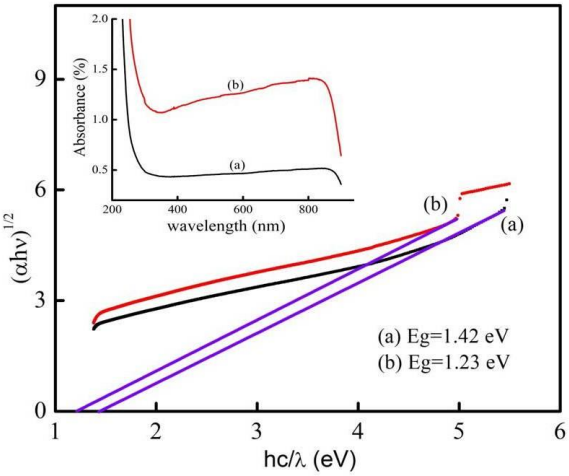


*Fig.4Tauc plot giving indirect bandgap for 2H $MoS_2$ (a) prepared as such and (b) annealed in vacuum at 300˚C and the lower inset shows corresponding absorption spectra.*

From the plot between $(\alpha h\nu)^{1/2}$ (as ordinate) and hv (as abscissa), and a straight line is obtained. Where $\alpha = 2.303 \log (A/d)$,is the absorption coefficient. The extrapolation of the straight line gives the value of the indirect band gap. The sample prepared as such shows a band gap of 1.42 eV and that of annealed sample is 1.23 eV. the sample shows a shift in absorbance edge and decrease in band gap during annealing. This can be explained as follows. With annealing the lattice of the material gets expanded and as a result the crystallite size increases. At the same time its band gap decreases with annealing. The decrease of band gap with increase in crystallite size can be attributed to quantum confinement.

## IV. CONCLUSION

Crystallite size obtained from Scherrer's equation and WH plot found to be increasing with annealing. This may be due to the lattice expansion. The lattice expansion is also confirmed by the tensile nature of strain and increase in c values of unit cell structures. The density also found to increases with annealing due to the process of densification in the annealed sample. The indirect band gap is found to be decreasing with increased crystallite size and this is the result of quantum confinement. Vaccum annealing preserves the phase and structure of the sulphide sample, which otherwise will get transformed to its oxide.

## V. ACKNOWLEDGMENT

All authors wish to acknowledge St.Thomascollege Pala, and CIF S.B.CollegeChanganassery and SAIF M.G.University for carrying out the various analysis reports for the samples.

## REFERENCES

[1]Chen, J., Li, S. L., Xu, Q., & Tanaka, K. (2002).Synthesis of open-ended MoS 2 nanotubes and the application as the catalyst of methanation. *Chemical Communications*, (16), 1722-1723.

[2]Lopez-Sanchez, O., Lembke, D., Kayci, M., Radenovic, A., &Kis, A. (2013). Ultrasensitive photodetectors based on monolayer MoS 2. *Nature nanotechnology*, *8*(7), 497-501.

[3]Wang, Q. H., Kalantar-Zadeh, K., Kis, A., Coleman, J. N., &Strano, M. S. (2012). Electronics and optoelectronics of two-dimensional transition metal dichalcogenides. *Nature nanotechnology*, *7*(11), 699-712.

[4]Manuja, M., Krishnan, S. V., & Jose, G. (2018).Molybdenum Disulphide nanoparticles synthesis using a low-temperature hydrothermal method and characterization. *Mater SciEng*, *360*, 012015-012015.

[5]Tsai, M. L., Su, S. H., Chang, J. K., Tsai, D. S., Chen, C. H., Wu, C. I., ...& He, J. H. (2014). Monolayer MoS2 heterojunction solar cells. *ACS nano*, *8*(8), 8317-8322.

[6] B. Chakraborty, R. Matte, A. K. Sood,C. N. R. Rao, Layer-dependent resonant Raman scattering of a few layer $MoS_2$, *Journal of Raman Spectroscopy*,44, 92 (2013).

[7]Gopalakrishnan, D., Damien, D., &Shaijumon, M. M. (2014).MoS2 quantum dot-interspersed exfoliated MoS2 nanosheets. *ACS nano*, *8*(5), 5297-5303.

[8]Umesh V Waghmare DM Singh, T Pradeep, JoydeepBhattacharjee The journal of physical chemistry. A 2005

[9]Quinn, M. D., Ho, N. H., &Notley, S. M. (2013).Aqueous dispersions of exfoliated molybdenum disulfide for use in visible-light photocatalysis. *ACS applied materials & interfaces*, *5*(23), 12751-12756.

[10] J. T. Lue, Physical properties of nanomaterials, Encyclopedia of nanoscience and nanotechnology, *American scientific publishers*, (2007).

[11]Manuja, M., Thomas, T., Jose, J., Jose, G., & George, K. C. (2019). Metal insulator transition driven by hydrated water of tungsten trioxide. *Journal of Alloys and Compounds*, *779*, 15-21.

[12]Manuja, M., Sarath, K. V., Thomas, T., Jose, J., & Jose, G. (2020).Effect of Structural Water on the Dielectric Properties of Hydrated Tungsten Trioxide. *Journal of Electronic Materials*, *49*(4), 2556-2567.

[13]Hwang, S. J., Petkov, V., Rangan, K. K., Shastri, S., &Kanatzidis, M. G. (2002). Structure of Nanocrystalline Materials with Intrinsic Disorder from Atomic Pair Distribution Function Analysis: The Intercalation Compound Ag x MoS2. *The Journal of Physical Chemistry B*, *106*(48), 12453-12458.

[14]Bandaru, N., Kumar, R. S., Sneed, D., Tschauner, O., Baker, J., Antonio, D., ...&Venkat, R. (2014). Effect of pressure and temperature on structural stability of MoS2. *The Journal of Physical Chemistry C*, *118*(6), 3230-3235.

[15]Chen, J. M., & Wang, C. S. (1974). Second order Raman spectrum of MoS2. *Solid State Communications*, *14*(9), 857-860.